Observation of an ultrahigh-temperature ferromagnetic-like transition in iron-contaminated multiwalled carbon nanotube mats

Guo-meng Zhao and Pieder Beeli
Department of Physics and Astronomy, California State University, Los Angeles, California 90032, USA
(Received 12 February 2008; revised manuscript received 5 May 2008; published 23 June 2008; publisher error corrected 27 June 2008)

We report magnetic measurements up to 1200 K on iron-contaminated multiwalled carbon nanotube mats with a Quantum Design vibrating sample magnetometer. Extensive magnetic data consistently show a ferrromagnetic transition at about 1000 K and a ferromagnetic-like transition at about 1275 K. The ferromagnetic transition at about 1000 K is associated with an Fe impurity phase and its saturation magnetization is in quantitative agreement with the Fe concentration measured by an inductively coupled plasma mass spectrometer. On the other hand, the saturation magnetization for the ferromagnetic-like phase (at 1275 K) is about 4 orders of magnitude larger than that expected from the measured concentration of Co or CoFe. We show that this ultrahigh-temperature ferromagnetic-like (UHTFL) transition is not consistent with ferromagnetism of any Fe-carbon phases, carbon-based phases, or magnetic impurities. Alternatively, the observed magnetic behavior of the UHTFL phase is phenomenologically explained in terms of the paramagnetic Meissner effect (orbital ferromagnetism) due to the existence of π Josephson junctions in a granular superconductor.

DOI: 10.1103/PhysRevB.77.245433 PACS number(s): 75.30.Cr, 74.25.Ha, 61.48.De

There are reports of intrinsic weak ferromagnetism in graphite and carbon-based materials well above room temperature,[1–4] as well as a theoretical prediction of a ferromagnetic instability in graphene sheets.[5] On the other hand, Talyzin *et al.*[6] showed that the observed high-temperature ferromagnetism in rhombohedral C_{60} (Ref. 7) is not intrinsic but caused by contamination of magnetic impurities. There are also several reports of high-temperature superconductivity in carbon films,[8,9] carbon nanotubes,[10] and graphite or graphite-sulfur composite.[2,3,11] Gonzalez *et al.*[12] showed that both high-temperature ferromagnetic and *p*-wave superconducting instabilities can occur in defective regions of graphite, where topological disorder enhances the density of states. Schrieffer[13] predicted ultrahigh-temperature superconductivity at a quantum critical point where ferromagnetic fluctuations are the strongest. Lee and Mendoza[14] showed that superconductivity as high as 500 K can be achieved through the pairing interaction mediated by undamped multiple acoustic plasmon modes in a quasi-one-dimensional electronic system.

Here we report magnetic measurements up to 1200 K on iron-contaminated multiwalled carbon nanotube mats. Our extensive magnetic data consistently show a ferrromagnetic transition at about 1000 K due to an Fe impurity phase and a ferromagnetic-like transition at about 1275 K. We show that this ultrahigh-temperature (1275 K) ferromagnetic-like (UHTFL) transition is not consistent with ferromagnetism of any Fe-carbon phases, carbon-based phases, or magnetic impurities. Alternatively, the observed magnetic behavior of the ultrahigh-temperature ferromagnetic-like phase is phenomenologically explained in terms of the paramagnetic Meissner effect (PME) (orbital ferromagnetism) due to the existence of π Josephson junctions in a granular superconductor.

Purified multiwalled nanotube (MWNT) mat samples are obtained from SES Research of Houston. Two different samples (Lot Nos. RS0656 and RS0657) were prepared by chemical vapor deposition using an iron catalyst. By burning off carbon-based materials in air, we find the weights of the residuals to be 2.25% and 1.73% for RS0656 and RS0657, respectively. On the assumption that the residual contains Fe_2O_3, Co_mO_n, and Ni_pO_q (where m, n, p, and q are integers), we determine the relative metal concentrations of the residual using a Perkin–Elmer Elan-DRCe inductively coupled plasma mass spectrometer (ICP-MS). Since the Co and Ni concentrations are negligibly small, the relative metal contents are nearly independent of the valences of Co and Ni we choose for their oxides. From the ICP-MS result and the weight of the residual, we obtain the metal-based magnetic impurity concentrations (ppm in weight) for RS0656, Fe =5340, Co=0.5, and Ni=13.7, and for RS0657, Fe=6940, Co=36.1, and Ni=20.5.

Magnetization was measured by a Quantum Design vibrating sample magnetometer (VSM). As checked by the Curie temperatures of both Ni and Fe, the absolute uncertainty of the temperature is less than 10 K. Figure 1(a) shows the temperature dependence of the susceptibility in a field of 2 Oe for a virgin MWNT mat sample (RS0657). This virgin sample was inserted into the sample chamber without going through the linear motor used for vibrating the sample. A 2 Oe field (using the ultralow-field option) was then applied after the sample was inserted. From the initial warming data, we clearly see a dip feature at about 833 K, which is caused by the competition between the ferrimagnetic transition (at about 860 K) of the Fe_3O_4 impurity phase and the decomposition of Fe_3O_4 into the higher Curie temperature α-Fe phase facilitated by the high vacuum inside the sample chamber (better than 9×10^{-6} torr). From the subsequent cooling and warming data, we see that the Curie temperature (T_C) of the Fe impurity is about 1000 K, which is lower than that (1047 K) for the bulk pure α-Fe. This is possibly due to the doping of carbon into Fe, which can significantly lower T_C.[15]

From Fig. 1(a), it is also apparent that a substantial low-field susceptibility (about 2.3×10^{-4} emu/g) persists up to 1100 K. Naturally, one is inclined to attribute this behavior to ferromagnetism originating from the Co ($T_C\simeq1400$ K) or CoFe ($T_C\simeq1250$ K) impurity phase. However, it is interest-

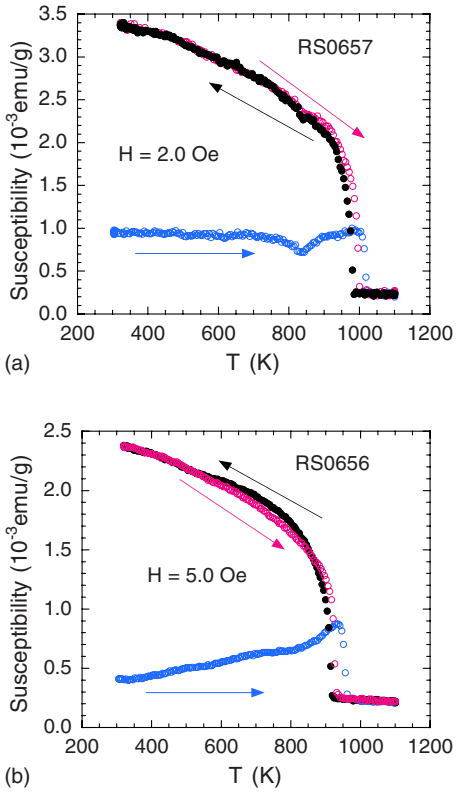

FIG. 1. (Color online) (a) Temperature dependence of the susceptibility in a field of 2 Oe for a virgin MWNT mat sample of RS0657 where the metal-based magnetic impurity concentrations (ppm in weight) are Fe=6940, Co=36.1, and Ni=20.5. (b) Temperature dependence of the susceptibility in a field of 5 Oe for a virgin MWNT mat sample of RS0656 where the metal-based magnetic impurity concentrations (ppm in weight) are Fe=5340, Co =0.5, and Ni=13.7. The susceptibility at 320 K appears to be proportional to the Fe concentration, while the susceptibility at 1100 K is independent of the Co concentration.

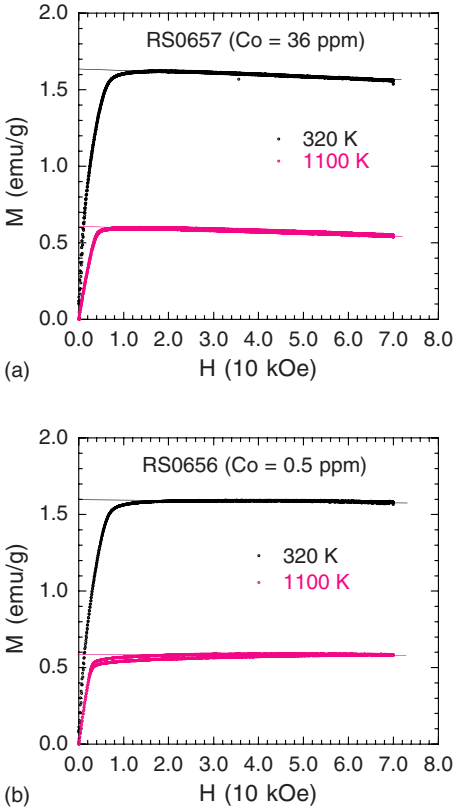

FIG. 2. (Color online) (a) Magnetization vs magnetic field at 320 and 1100 K for sample RS0657 where the Co concentration is 36.1 ppm. (b) Magnetization vs magnetic field at 320 and 1100 K for sample RS0656 where the Co concentration is 0.5 ppm. The saturation magnetization at 1100 K is independent of the Co concentration.

ing that this same magnitude of susceptibility is also seen in sample RS0656 [see Fig. 1(b)] where the Co concentration is only 0.5 ppm, almost 2 orders of magnitude less. Further, the concentration of Co (0.5 ppm) or CoFe (about 1 ppm) is *over 3 orders of magnitude*, too small to explain the measured susceptibility.[16] Therefore, this observed large susceptibility well above T_C of the Fe impurity phase cannot originate from a Co or CoFe impurity phase.

In Fig. 2(a), we plot magnetization vs magnetic field at 320 and 1100 K for sample RS0657, which were measured after the above low-field measurements. The coercivity H_c is about 140 Oe at 320 K and is negligibly small at 1100 K. The saturation magnetizations (M_s) are 1.63 emu/g at 320 K and 0.60 emu/g at 1100 K. It is clear that M_s at 1100 K is substantial, indicating a second magnetic transition above 1100 K. This second UHTFL phase cannot be associated with the Co (or CoFe) impurity phase whose concentration is only 36.1 ppm (or 72 ppm) in this sample. Such a small Co or CoFe impurity concentration can contribute a saturation magnetization of $<1.0\times10^{-2}$ emu/g (see Ref. 16), which is about 2 orders of magnitude smaller than the measured value (0.63 emu/g). For sample RS0656, which contains 5340 ppm Fe impurity and 0.5 ppm Co impurity, M_s are 1.60 emu/g at 320 K and 0.59 emu/g at 1100 K [see Fig. 2(b)]. These M_s values for sample RS0656 are very similar to those for sample RS0657. The measured M_s at 1100 K for sample RS0656 is about *4 orders of magnitude* larger than the value expected from the measured Co or CoFe impurity concentration. This definitively excludes a Co or CoFe impurity phase from being the origin of the UHTFL behavior.

Since the magnetization in 20 kOe is close to the saturation magnetization (see Fig. 2), the temperature dependence of the saturation magnetization is approximated by the temperature dependence of the magnetization in 20 kOe. In Fig. 3(a), we plot the temperature dependence of the magnetization in a field of 20 kOe for another virgin sample of RS0657. One can clearly see that the magnetization above the Curie temperature of the Fe impurity phase is large up to 1200 K, implying that the transition temperature of the UHTFL phase is higher than 1200 K. If we assume that the curve of $M_s(T)/M_s(0)$ versus T/T_C for this UHTFL phase is the same as that for Ni (see the solid line), we find T_C and $M_s(0)$ to be 1275 K and 0.97 emu/g, respectively. The saturation magnetization of the Fe impurity phase is then found to be about 0.57 emu/g at 320 K.

In Fig. 3(b), we show the temperature dependence of the magnetization in a field of 20 kOe for a thermally annealed sample of RS0657. This sample was annealed in air at

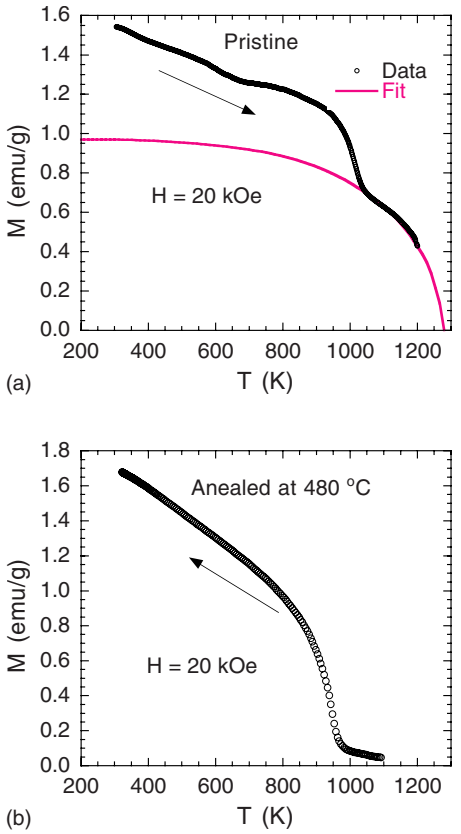

FIG. 3. (Color online) (a) Temperature dependence of the magnetization in a field of 20 kOe for a virgin MWNT mat sample of RS0657. The temperature dependence of the magnetization in 20 kOe should be similar to that of the saturation magnetization (M_s). The solid line is a fit using the curve of $M_s(T)/M_s(0)$ versus T/T_C for Ni, appropriately scaled to T_C=1275 K. (b) Temperature dependence of the magnetization in a field of 20 kOe for a thermally annealed sample of RS0657. This sample was annealed in air at 480 °C for about 5 min.

480 °C for about 5 min and its mass was measured about 1 h after it was cooled down to room temperature. The mass of the annealed sample was found to be smaller than that of the pristine sample by about 2%. This mass decrease may be due to the removal of amorphous carbon and/or the outershells of MWNTs. These data were taken after an *M-H* loop was measured at 1100 K. With such a high temperature and vacuum, all the Fe oxides have been converted to α-Fe. It is remarkable that the magnetization at 1100 K is reduced by 1 order of magnitude compared to that for the pristine sample [see Fig. 3(a)] while the magnetization at 320 K increases by about 10%.

Figure 4 shows the temperature dependence of the magnetization in a field of 20 kOe for the residual of sample RS0657, which is obtained by burning off carbon-based materials in air at 550 °C for about 10 min. The data were similarly taken after an *M-H* loop was measured at 1100 K. The specific magnetization is calculated using the mass of the pristine MWNT mat sample. As indicated by the arrow, the ferromagnetic transition temperature is about 1037 K which is the same as T_C of α-Fe if one considers a thermal lag of about 10 K. Consistent with the two phase model of

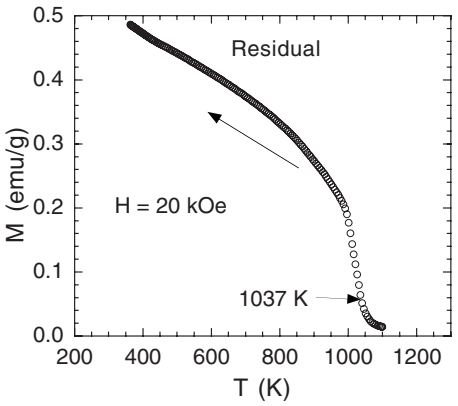

FIG. 4. Temperature dependence of the magnetization in a field of 20 kOe for the residual of sample RS0657, which was obtained by burning off carbon-based materials in air at 550 °C for about 10 min. The specific magnetization is calculated using the mass of the pristine MWNT mat sample.

Fig. 3(a), the magnetization of the residual at 320 K is three times smaller than that for the annealed sample containing MWNT mats [Fig. 3(b)]. This implies a giant enhancement of the magnetization of the Fe impurity due to the presence of MWNTs. It is interesting that such a giant enhancement of the saturation magnetization was also observed in one of the Canyon Diablo graphite nodule samples (see the results for sample 1.1 of Ref. 17).

From *M-H* loop measurements of the residual, we find the saturation magnetizations at 320 and 1100 K to be 0.52 and 4.5×10^{-3} emu/g, respectively. The M_s value of the α-Fe impurity at 320 K inferred from the data of the residual is in excellent agreement with that (0.57 emu/g) inferred from the data of the pristine sample [(Fig. 3(a)]. If we calculate M_s using the mass of the Fe impurity in the residual, we find M_s to be 74.9 emu/g of Fe in agreement with the value used in Ref. 17. Our magnetic measurements on Fe_3O_4 nanoparticles with an average diameter of 40–60 nm also show that M_s =77.0 emu/g of Fe at 320 K after the decomposition of Fe_3O_4 into Fe via a thermal cycle up to 1100 K in high vacuum. This implies that the M_s value of Fe nanoparticles is significantly smaller than the bulk value (~200 emu/g), which could be caused by spin disorder on the surface of nanoparticles.[18] Moreover, the measured M_s value at 1100 K (4.5×10^{-3} emu/g) is the same as the bulk M_s value at 1100 K (4.5×10^{-3} emu/g) calculated from the measured Co impurity concentration (36.1 ppm).[16] Such excellent consistencies between the magnetic data of the residual and the ICP-MS results further show that the UHTFL phase seen in Figs. 1, 2, and 3(a) is not associated with any magnetic impurity phase.

Now we discuss the origin of the UHTFL behavior. We entertain the possibility that the UHTFL behavior could arise from a magnetic proximity effect[17] in a coupled Fe-carbon system. Since our two phase (Fe and UHTFL) model produces a fit [Fig. 3(a)] where the Fe concentration is in quantitative agreement with that determined by both M_s value on the residual (Fig. 4) and the ICP-MS analysis, the majority of the Fe impurities must be isolated from carbon. This leaves only a very small fraction of the Fe impurities to couple

strongly with carbon to polarize the spins of carbons such that the saturation magnetization of the coupled system increases enormously from that of isolated Fe. One imagines that an annealing procedure could destroy this Fe-carbon coupling so that the magnetization of the UHTFL phase would then be removed both above and below T_C of Fe. This is in contradiction with Fig. 3(b) where the sharp decrease in magnetization above T_C of Fe does not have a corresponding decrease in magnetization below T_C. For the same reason, the UHTFL behavior cannot originate from ultrahigh-temperature ferromagnetism of any unknown Fe-carbon phase with an M_s many times larger than that of isolated Fe. A third possibility is that MWNTs and/or an unknown carbon phase are ferromagnetic with an ultrahigh Curie temperature (1275 K). This interpretation is very unlikely because, as with our magnetic proximity-effect scenario, the saturation magnetization of any ferromagnetic carbon would be removed both above and below T_C of Fe when the ferromagnetic phase was destroyed by an annealing procedure. Finally the same argument used to rule out ferromagnetic carbon can also be used to rule out any non-Fe-based magnetic phase as the origin of the UHTFL behavior.

It is clear that the comparisons among Figs. 3(a), 3(b), and 4 rule out interpretations based on ultrahigh-temperature ferromagnetism of any carbon-based phases, Fe-carbon phases, or magnetic impurities. Alternatively, if MWNTs are superconducting, a MWNT mat should be a granular superconductor. The existence of magnetic impurities in the Josephson network should lead to the formation of π junctions with a negative Josephson coupling energy J.[19] If the critical current is large enough, an odd number of π junctions within a loop generates a spontaneous orbital moment (a fractional quantum flux) associated with the circulation current around the loop.[20,21] The interaction of these orbital moments can lead to ferromagnetic-like ordering (orbital ferromagnetism), which is the origin of the PME.[20] Since the diameters of nanotubes are comparable to the magnetic penetration depth,[10] the diamagnetic Meissner effect is negligibly small so that magnetic field can enter into the Josephson-coupled network even in a zero-field-cooled condition. Since π junctions can be formed even if the impurities are not in the ferromagnetic state,[19] the ferromagnetic-like ordering of the orbital moments can occur above the Curie temperature of the magnetic impurities. This can explain the data shown in Fig. 3(a), where the transition at 1275 K is associated with the onset of the PME. On the other hand, if the Josephson coupling is substantially reduced by the removal of the outershells of MWNTs after annealing in air at 480 °C, the critical current might not be large enough to sustain a spontaneously generated vortice within a π loop when the magnetic impurities are in the paramagnetic state. Then the orbital moments associated with the spontaneously generated vortices will be significantly reduced above T_C of the magnetic impurities. On the other hand, if some ferromagnetic impurities are inside the π loops, the large magnetization of magnetic impurities below T_C can greatly enhance the stability of the spontaneous vortex state due to a large decrease in the magnetic energy compared with that for the nonvortex state. This picture naturally explains the result in Fig. 3(b) where the saturation magnetization of the UHTFL phase is restored just below T_C of the Fe impurity phase. We thus observe a symbiotic relationship between the magnetic impurities and the magnetic behavior of our superconducting MWNT mat. A more quantitative explanation based on the model in Ref. 20 will be given elsewhere. If the PME is the only plausible interpretation, our present results imply ultrahigh-temperature superconductivity in MWNT mat samples.

If the interpretation based on the paramagnetic Meissner effect is relevant, there should be other signatures of superconductivity in carbon nanotubes. Zhao and Wang[10] showed over 20 independent signatures of superconductivity including the resistive superconducting transition, nearly zero on-tube resistance at room temperature in individual MWNTs, and large single-particle excitation gaps in both single-walled nanotubes (100–150 meV) and MWNTs (about 200 meV). While previous high-temperature superconductors of the late 1980s and early 1990s have quickly exhibited the thermal coincidence of a near 100% diamagnetic Meissner fraction with the zero resistance state, one must recognize that these are bulk signatures and our MWNTs are nanosize materials. If our MWNTs are superconductors they cannot exhibit these traditional bulk signatures. For example, the on-tube resistance of individul tubes will never go to zero due to significant thermally activated and quantum phase slips in this quasi-one-dimensional superconductor with a small number of transverse conduction channels. Similarly, because the diameters of our tubes are less than the penetration depth (see below), the diamagnetic Meissner effect is expected to be small. Nevertheless, one should be able to observe this small diamagnetic Meissner effect if the superconducting tubes are free of magnetic contaminants so that the paramagnetic Meissner effect is no longer pronounced. Since the orbital diamagnetic susceptibility in a magnetic field perpendicular to tubes' axes is large, it is difficult to separate the Meissner effect from the large orbital diamagnetic susceptibility. On the other hand, the orbital susceptibility in a magnetic field parallel to tubes' axes is predicted to be very small at room temperature,[22] similar to the case of graphite in a field parallel to the plane. This makes it possible to extract the Meissner effect from the measured susceptibility in a parallel field.

Figure 5 shows the temperature dependence of the susceptibility for aligned MWNTs in a magnetic field parallel to the tubes' axes. The data for physically separated (PS) tubes are from Ref. 23 and the data for physically coupled bundles are from Ref. 24. Although the average diameters of these tubes are similar (about 10 nm),[23,25] it is apparent that the diamagnetic susceptibility of physically separated tubes is quite different from that of physically coupled bundles. Because the orbital diamagnetic susceptibility in the parallel field is calculated to be negligible at room temperature,[22] the observed large diamagnetic susceptibility just above 265 K is difficult to explain if these tubes are not superconductors.

We can quantitatively explain the observed large diamagnetic susceptibility (-0.8×10^{-5} emu/g) at 265 K for the physically separated tubes if we attribute it to the diamagnetic Meissner effect due to superconductivity. For physically separated superconducting tubes in a magnetic field parallel to the tubes' axes, the diamagnetic susceptibility due to the Meissner effect is given by

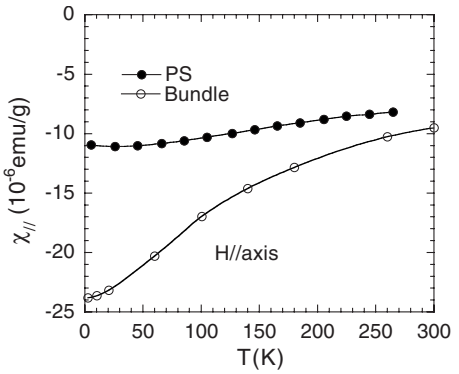

FIG. 5. Temperature dependence of the susceptibility for aligned MWNTs in a magnetic field parallel to the tube's axis. The data for physically separated (PS) tubes are from Ref. 23 and the data for physically coupled bundles are from Ref. 24. These nanotubes were produced using a catalyst-free arc-discharge method.

$$\chi_{\parallel}^{S}(T) = -\frac{\bar{r}^2}{32\pi\lambda_{\theta}^2(T)}. \quad (1)$$

Here r is the radius of a tube, $\bar{r}^2$ is the average value of r^2, and $\lambda_\theta(T)$ is the penetration depth when carriers move along the circumferential direction. The above equation is valid only if $\lambda_\theta(0)$ is larger than the maximum radius of the tubes, which is the case for our MWNTs (see below). Equation (1) indicates that the Meissner effect is inversely proportional to $1/\lambda_\theta^2(T)$. Since $T_{c0} > 1275$ K, $1/\lambda_\theta^2(T)$ and thus $\chi_{\parallel}^{S}(T)$ are nearly independent of temperature below 265 K. Then we have $\chi_{\parallel}^{S}(0) \simeq \chi_{\parallel}^{S}(265\ \mathrm{K}) = -0.8\times10^{-5}$ emu/g. If we assume that the radii of tubes have a Gaussian distribution, $\exp[-(r-50)^2/25^2]$, we find $\bar{r}^2 = 2801$ Å^2. With the weight density of 2.17 g/cm^3 (Ref. 26) and $\chi_{\parallel}^{S}(0) = -0.8\times10^{-5}$ emu/g, we calculate $\lambda_\theta(0) \simeq 1265$ Å. This value of the penetration depth corresponds to $n/m_\theta^* = 1.77\times10^{21}/\mathrm{cm}^3 m_e$, where n is the carrier density and m_θ^* is the effective mass of carriers along the circumferential direction. If we take $m_\theta^* = 0.012 m_e$, which is typical for graphites,[27] we estimate $n = 2.12\times10^{19}/\mathrm{cm}^3$, in quantitative agreement with a Hall-effect measurement[28] which gives $n = 1.6\times10^{19}/\mathrm{cm}^3$.

From Eq. (1), we can see that $|\chi_{\parallel}^{S}(T)|$ will increase linearly with increasing $\bar{r}^2$. For Josephson-coupled MWNT bundles, the effective $\bar{r}^2$ is larger than that for physically separated tubes. As the temperature decreases, the Josephson coupling strength increases so that the effective $\bar{r}^2$ and $|\chi_{\parallel}^{S}(T)|$ also increase. This can naturally explain why the diamagnetic susceptibility for physically coupled MWNTs is larger than that for physically separated MWNTs and why the enhancement in the diamagnetic susceptibility increases significantly with decreasing temperature (see Fig. 5). At the lowest temperature, the enhancement factor is over 2. Without invoking superconductivity in these MWNTs, it is very difficult to account for such a large enhancement in the diamagnetic susceptibility upon bundling of the tubes.

In summary, we report magnetic measurements up to 1200 K on iron-contaminated multiwalled carbon nanotube mats. Extensive magnetic data consistently show a ferrromagnetic transition at about 1000 K and a ferromagnetic-like transition at about 1275 K. The ferromagnetic transition at about 1000 K is associated with an Fe impurity phase and its saturation magnetization is in quantitative agreement with the Fe concentration measured by an inductively coupled plasma mass spectrometer. On the other hand, the saturation magnetization for the ferromagnetic-like phase (at 1275 K) is about 4 orders of magnitude larger than that expected from the measured concentration of Co or CoFe. We show that this ultrahigh-temperature ferromagnetic-like transition is not consistent with ferromagnetism of any Fe-carbon phases, carbon-based phases, or magnetic impurities. Alternatively, the observed magnetic behavior of ultrahigh-temperature ferromagnetic-like phase can be consistently explained in terms of the paramagnetic Meissner effect (orbital ferromagnetism) due to the existence of π Josephson junctions in a granular superconductor.

We thank M. Du, G. Gao, and F. M. Zhou in the Department of Chemistry and Biochemistry at CSULA for the elemental analyses using ICP-MS. We also thank the Palmdale Institute of Technology for the use of the VSM and Lockheed Martin Aeronautics for the cryogens. This research is partly supported by a Cottrell Science Award from Research Corporation.

[1] D. Mendoza, F. Morales, R. Escudero, and J. Walter, J. Phys.: Condens. Matter **11**, L317 (1999).
[2] Y. Kopelevich, P. Esquinazi, J. H. S. Torres, and S. Moehlecke, J. Low Temp. Phys. **119**, 691 (2000).
[3] S. Moehlecke, C. Ho, and M. B. Maple, Philos. Mag. B **82**, 1335 (2002).
[4] K. Murata, H. Ushijima, H. Ueda, and K. Kawaguchi, J. Chem. Soc., Chem. Commun. **7**, 567 (1992).
[5] G. Baskaran and S. A. Jafari, Phys. Rev. Lett. **89**, 016402 (2002).
[6] A. Talyzin, A. Dzwilewski, L. Dubrovinsky, A. Setzer, and P. Esquinazi, Eur. Phys. J. B **55**, 57 (2007).
[7] T. Makarova, B. Sundqvist, R. Hohne, P. Esquinazi, Y. Kopelevich, P. Scharff, V. A. Davydov, L. S. Kashevarova, and A. V. Rakhmanina, Nature (London) **413**, 716 (2001).
[8] K. Antonowicz, Nature (London) **247**, 358 (1974).
[9] S. G. Lebedev, Nucl. Instrum. Methods **A521**, 22 (2004); S. G. Lebedev, Priroda (Sofia) **N8**, 38 (2007).
[10] G. M. Zhao and Y. S. Wang, arXiv:cond-mat/0111268 (unpublished); G. M. Zhao, *Trends in Nanotubes Research*, edited by Delores A. Martin (Nova Science, New York, 2006), pp. 39–75, and references therein.
[11] R. R. da Silva, J. H. S. Torres, and Y. Kopelevich, Phys. Rev. Lett. **87**, 147001 (2001).
[12] J. Gonzalez, F. Guinea, and M. A. H. Vozmediano, Phys. Rev. B **63**, 134421 (2001).

[13] J. R. Schrieffer, J. Supercond. Novel Magn. **17**, 539 (2004).
[14] Y. C. Lee and B. S. Mendoza, Phys. Rev. B **39**, 4776 (1989).
[15] E. M. Terry, Phys. Rev. (Series I) **30**, 133 (1910).
[16] The low-field susceptibility of spherical Co or CoFe particles is $3/4\pi$ emu/cm^3=0.031 emu/g. The bulk saturation magnetization M_s of Co at 1100 K is calculated to be 125 emu/g from the value (162 emu/g) of M_s at room temperature and T_C =1404 K using the normalized temperature dependence of M_s for Ni; For bulk CoFe, M_s at 1100 K is estimated to be 141 emu/g. The T_C and bulk M_s at room temperature of Co and CoFe can be found at http://www.irm.umn.edu/hg2m/hg2m??b/hg2mb.html.
[17] J. M. D. Coey, M. Venkatesan, C. B. Fitzgerald, A. P. Douvalis, and I. S. Sanders, Nature (London) **420**, 156 (2002).
[18] J. Restrepo, Y. Labaye, and J. M. Greneche, Physica B (Amsterdam) **384**, 221 (2006).
[19] B. I. Spivak and S. A. Kivelson, Phys. Rev. B **43**, 3740 (1991).
[20] F. V. Kusmartsev, Phys. Rev. Lett. **69**, 2268 (1992).
[21] D. Dominguez, E. A. Jagla, and C. A. Balseiro, Phys. Rev. Lett. **72**, 2773 (1994).
[22] J. P. Lu, Phys. Rev. Lett. **74**, 1123 (1995); Figure 4 of this reference indicates that the magnitude of the susceptibility in the parallel field (square and diamond symbols) becomes negligibly small when $k_BT > 0.3\Delta_o = 1.1$ eV Å$/r$. Since the orbital susceptibility is proportional to r, the outermost shell in a MWNT contributes the most to the orbital susceptibility. Then for the average radius of 50 Å of these MWNTs, the orbital susceptibility is negligible when $k_BT > 1.1$ eV Å/(50 Å)=22 meV. Therefore, the orbital susceptibility is negligible at room temperature where k_BT=25.6 meV.
[23] O. Chauvet, L. Forro, W. Bacsa, D. Ugarte, B. Doudin, and W. A. de Heer, Phys. Rev. B **52**, R6963 (1995). The aligned nanotube films were produced by a process in which the tubes are ultrasonically separated.
[24] X. K. Wang, R. P. H. Chang, A. Patashinski, and J. B. Ketterson, J. Mater. Res. **9**, 1578 (1994).
[25] S. N. Song, X. K. Wang, R. P. H. Chang, and J. B. Ketterson, Phys. Rev. Lett. **72**, 697 (1994). The MWNT bundles used in this work are the same as those in Ref. 24.
[26] D. Qian, E. C. Dickeya, R. Andrews, and T. Rantell, Appl. Phys. Lett. **76**, 2868 (2000).
[27] V. Bayot, L. Piraux, J.-P. Michenaud, and J.-P. Issi, Phys. Rev. B **40**, 3514 (1989).
[28] G. Baumgartner, M. Carrard, L. Zuppiroli, W. Bacsa, W. A. de Heer, and L. Forro, Phys. Rev. B **55**, 6704 (1997).